Long-Term 30-Year Variation (1990s-2020) of Background Tropospheric Ozone Concentration at Japanese Remote Stations

Itahashi, Syuichi
Research Institute for Applied Mechanics (RIAM), Kyushu University

出版情報：SOLA. 21, pp.94-100, 2025. 日本気象学会
バージョン：

Long-Term 30-Year Variation (1990s−2020) of Background Tropospheric Ozone Concentration at Japanese Remote Stations

Syuichi Itahashi

Research Institute for Applied Mechanics (RIAM), Kyushu University, Kasuga, Fukuoka, Japan

(Manuscript received 11 November 2024, accepted 24 December 2024)

Abstract Tropospheric ozone (O_3) is an air pollutant and greenhouse gas and is still a problem in East Asia. O_3 is formed via secondary photochemistry from nitrogen oxide (NO_x) and volatile organic compound (VOC) precursors. Because of the increase in anthropogenic emissions globally, changes in O_3 concentration over the Northern Hemisphere have been a concern. In this study, using measurements at three remote sites conducted by the Japan Meteorological Agency (JMA), the 30-year (1990s to 2020) long-term trend of background O_3 concentration was analyzed. The results of the fitted curve revealed that background O_3 concentration has changed by within ±0.3 ppbv/year over 30 years. The increasing trend at Ryori (39.03°N, 141.82°E) peaked in 2009 and then decreased, agreeing well with other reports in the mid-latitude zone (40°N–55°N). In contrast, the present study revealed continuous decreasing trends at Minamitorishima (24.28°N, 153.98°E) and Yonagunijima (24.47°N, 123.02°E) at lower latitudes. In addition, the analysis for 2020 clarified that the frequency density shifted to a lower O_3 concentration compared with the dataset for the 1990s to 2019 at all three remote sites in Japan. This suggested that the emission reduction resulting from the COVID-19 pandemic could be a factor causing the decreasing background O_3 concentration.

Citation: Itahashi, S., 2025: Long-term 30-year variation of background tropospheric ozone concentration at Japanese remote stations. *SOLA*, **21**, 94−100, doi:10.2151/sola.2025-012.

1. Introduction

Tropospheric ozone (O_3) is an air pollutant and greenhouse gas that is produced via photochemical reactions of nitrogen oxide (NO_x) and volatile organic compound (VOC) precursors (Seinfeld and Pandis 2016). Because of the growing anthropogenic emissions of NO_x and VOCs since the 1970s (Kurokawa and Ohara 2020; Crippa et al. 2018, 2023), O_3 pollution, particularly over the Northern Hemisphere, has been a major concern. Given its long lifetime, O_3 can be long-range transported away from source regions, for example, from one continent to another (Guerova et al. 2006; Itahashi et al. 2020; Mathur et al. 2022). Thus, O_3 is not only a pollutant on a local scale near intense emission sources, but also a pollutant on hemispheric scales. In this manner, measurements taken at sites least affected by local emission sources can give an indication of background O_3 concentration. The background O_3 levels appeared to have approximately doubled, with the greatest increase since the 1950s, and annual average background O_3 concentration over the mid-latitudes of the Northern Hemisphere has ranged from 20 to 45 ppb (Vingarzan 2004). Long-term measurement data over Europe (beginning in the 1950s and before), North America (beginning in 1984), and Asia (beginning in 1991) show that O_3 has increased at all sites in all seasons at approximately 1%/year relative to the level in 2000 (Parrish et al. 2012). The updated study suggested that the increasing O_3 trend has ended, with a maximum concentration reached in the mid-2000s, followed by slow decrease in Europe and North America (Parrish et al. 2020). The exception to this peak-out trend was found at the Asian site of Mt. Waliguan (36.28°N, 100.90°E, 3.8 km) in Qinghai Province, China.

Because long-range O_3 transport is a concern, the effects of the Asian continent on the downwind region of Japan have been investigated in previous studies (Itahashi et al. 2013, 2015; Chatani et al. 2020; Itahashi 2023). The background O_3 concentration in the early 1990s was estimated as 35–40 ppbv (Akimoto et al. 1996), although the background O_3 concentration in Japan was estimated as higher than the background concentration over the USA and Europe in 1980s (Sunwoo et al. 1994). The 8-year (1989–1997) ozonesonde data at Okinawa, southern Japan, showed an increasing trend of 2.5 ± 0.6%/year (Lee et al. 1998). The O_3 trend from 1998 to 2006 at Mt. Happo (36.70°N, 137.80°E, 1.9 km) during springtime, when dominated by the East Asian continental outflow, showed growth of +1 ppbv/year (Tanimoto 2009). The numerical model simulation also highlighted the impact of O_3 from outside of Japan on these increasing trends (Nagashima et al. 2017). The O_3 trends at Japanese monitoring sites mostly in urban areas have been analyzed from 1980 to 2015, and the analysis suggested that photochemical production and the weakening NO titration effect because of the reduction in NO_x emissions increased O_3 concentration (Kawano et al. 2022). The development of a historical emission inventory and subsequent model simulation during 2000–2019 indicated that emission regulation

Corresponding author: Syuichi Itahashi, Research Institute for Applied Mechanics, Kyushu University, Kasuga, Fukuoka 816-8580, Japan.
E-mail: syuichi@riam.kyushu-u.ac.jp.

in Japan partly led to the increase of annual mean O_3 because of weakening NO titration; however, the regulation suppressed high O_3 concentrations (Chatani et al. 2023). Although there are many previous studies discussing O_3 pollution status in Japan, the background O_3 concentration in Japan has not been well examined. In addition, O_3 pollution in 2020, when human activities were severely restricted by COVID-19, should be analyzed for background O_3 concentration because previous research focused mainly on O_3 variation over urban areas. Therefore, in the present work, we analyzed an O_3 concentration measurement dataset at three remote sites in Japan from the 1990s to 2020, and we report the long-term 30-year trend and its change in 2020.

2. Dataset

The Japan Meteorological Agency (JMA) conducted the greenhouse gas measurements at three remote sites, and O_3 has been measured since the 1990s (JMA 2024). Figure 1 shows these sites. Minamitorishima (MNM) is an island in the North Pacific Ocean, in easternmost Japan (24.28°N, 153.98°E, 7 m above sea level (a.s.l.)), at which O_3 measurements started in January 1994. Yonagunijima (YON) is an island in westernmost Japan (24.47°N, 123.02°E, 30 m a.s.l.), at which O_3 measurements started from January 1997. Ryori (RYO) is located on a hilly cape on the Pacific coast of northeast Japan (39.03°N, 141.82°E, 260 m a.s.l.), at which O_3 measurements started in January 1990. All three sites are highly suitable for background O_3 measurements because the local emissions are negligible (e.g., Itahashi et al. 2021, 2024). Air samples were introduced into the measuring system from the inlet on the measurement room's roof with a flow rate of 10 L/min. The inlet was 8 m from the ground at MNM and RYO, and 10 m at YON. The measuring system for O_3 consisted of an ultraviolet (UV) absorption monitor that measured O_3 concentrations every 10 s. The hourly data were calculated by the arithmetic mean of all measured data over 1 h after removing irregular data and evident errors. The calibration for the UV O_3 monitor was normally done twice a year based on the calibration system at JMA Headquarters in Tokyo. Monitoring sites with more than 6000 h (corresponding to 250 days) of measurement time are considered effective measuring sites and evaluated as meeting the Japanese environmental quality standard. In this study, we also applied this criterion for the data from MNM, YON, and RYO. The data from RYO in 1990 and 1991 were excluded from the analysis based on this criterion.

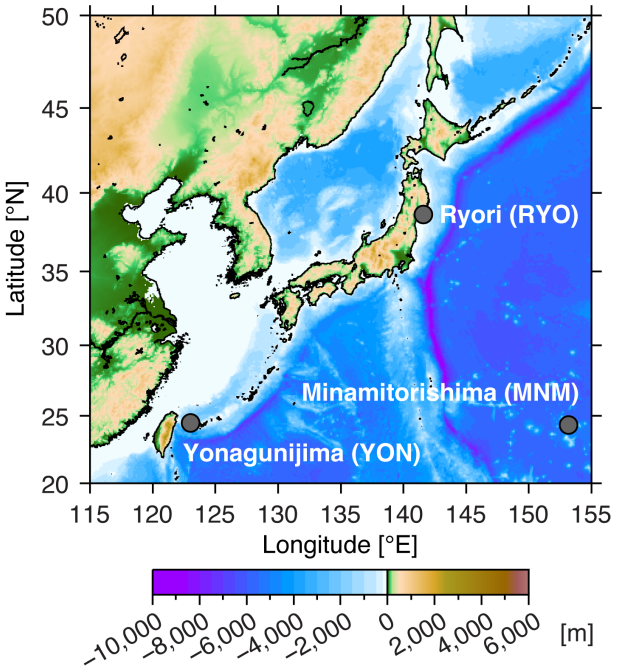

Fig. 1. Geographical map of JMA measurement stations at Minamitorishima (MNM), Yonagunijima (YON), and Ryori (RYO).

3. Results and discussion

All long-term background O_3 concentrations at MNM, YON, and RYO are shown in Fig. 2. At MNM (Fig. 2a), annual mean O_3 concentrations were in the range of 25–35 ppbv, and the median was generally lower than annual mean. The maximum values exceeded 70 ppbv in some years, even at a remote site in the northwest Pacific Ocean. At YON (Fig. 2b), annual mean concentrations were around 40 ppbv, and the median was greater than annual mean. The maximum value exceeded 100 ppbv, which could be affected by the outflow from the Asian continent (i.e., Itahashi et al. 2024). At RYO (Fig. 2c), the annual mean and the median were close and these values were in the range of 35–40 ppbv during the analyzed period.

These datasets were decomposed into the monthly and annual mean data, and then the long-term trends were analyzed following the approach described by Parrish et al. (2019, 2020) for the monthly mean. In this analysis, O_3 concentration ($[O_3]$) is expressed as the least-squares fits of Eq. (1).

$$[O_3] = a + bt + ct^2 + \text{residuals} \quad (1)$$

Parameters a, b, and c in the power series are the coefficients that quantify the O_3 concentration trend. Time origin t for this quadratic polynomial was chosen as the year 2000 (i.e., $t = 2000$ in Eq. (1)); therefore, coefficient a was the intercept of the fitted curve at 2000. Coefficient b was the slope of the fitted curve, quantifying the rate of change of O_3 concentration over time at the beginning of the year 2000. Finally, coefficient c was equal to one-half of the time rate of

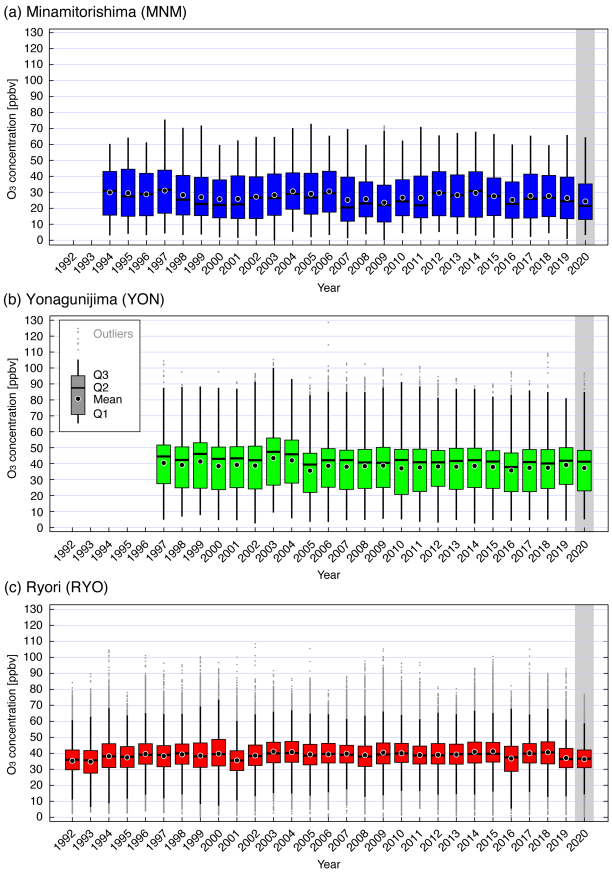

Fig. 2. Timeseries of all hourly measurement data during the analyzed period as box plots at (a) Minamitorishima, (b) Yonagunijima, and (c) Ryori. The lower and upper fences in the box plot are the 25th (Q1) and the 75th (Q3) percentiles and the thick line in the box plot is the 50th percentile (median) (Q2). The whiskers are defined as the minimum (Q1 − 1.5 interquartile range (IQR)) and the maximum (Q3 + 1.5 IQR) values where the IQR is Q3–Q1 and the gray dots are outliers of data beyond the minimum and maximum. The circle is the arithmetic mean. The gray shading indicates the year of the COVID-19 pandemic.

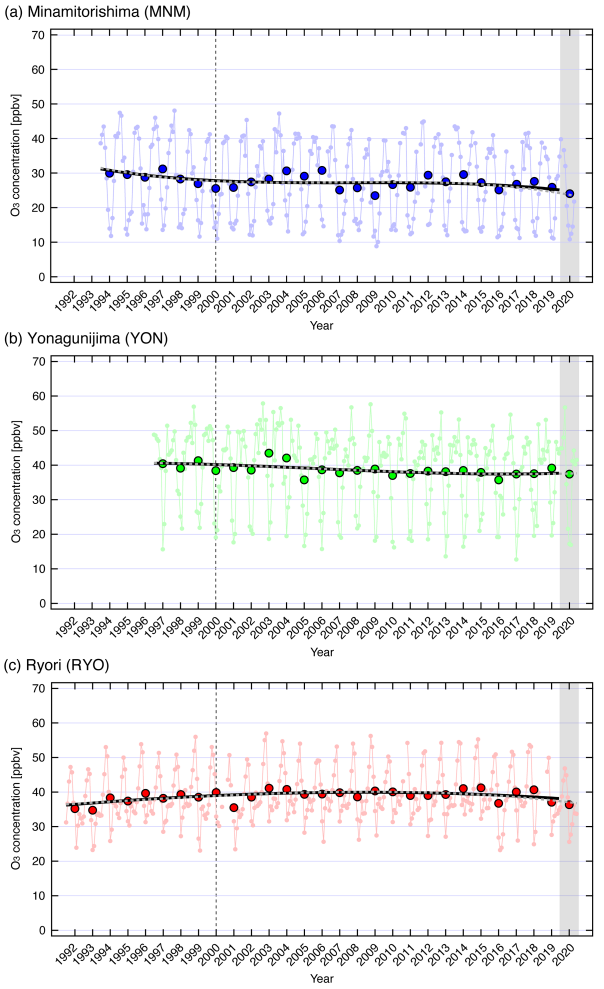

Fig. 3. Timeseries of monthly and annual mean O_3 at (a) Minamitorishima, (b) Yonagunijima, and (c) Ryori. The solid black curve represents the nonlinear, least squares regression fits of a quadratic polynomial to the monthly data from the 1990s to 2019 and the dotted gray curve is the result including the data in the year 2020. The gray shading indicates the year of the COVID-19 pandemic.

change of the fitted curve slope, indicating the acceleration or deceleration of the trend. The monthly and annual mean and the fitted curve for the monthly mean derived based on Eq. (1) are shown in Fig. 3, and the statistical results for the three parameters are listed in Table 1. Because of the larger variation in MNM and YON compared with RYO, the significance level of $p < 0.05$ was obtained only at RYO in this fitting curve analysis. The a values were 28.0, 40.3, and 38.9 ppbv at MNM, YON, and RYO, respectively (Table 1). The timeseries in Fig. 2 showed that O_3 concentration was lowest at MNM in the Pacific Ocean, whereas those at YON and RYO were higher concentration in 2000. The Pacific marine boundary layer on the US west coast had an a value of 32.9 ± 1.1 ppbv (Table 1 and detailed in Parrish et al. 2020), and the results at MNM in this study were similar. Moreover, the a value at Mace Head, Ireland was around 40 ppbv from the 1980s to the 2010s (Table 1 and detailed in Derwent et al. 2018 and Parrish et al. 2020), mostly consistent with those at YON and RYO in this study. The background O_3 concentration observed around Japan corresponded well to other reported values (e.g., Parrish et al. 2020). Coefficient b was negative at MNM and YON, indicating the decreasing trend for O_3, whereas b was positive at RYO. Negative slopes are not found at most observation sites in the Northern Hemisphere (Parrish et al. 2020), and this was a unique trend revealed in this study. One possible reason is the difference in latitude; the observation sites reported by Parrish et al. (2020) were at 40°N–55°N, whereas MNM and YON in this study were at 25°N. Although these results at MNM and YON were not significant ($p > 0.05$), the behavior at different latitudes in the Northern Hemisphere should be studied further. At RYO, which is at the same latitude as the site in the report by Parrish et al. (2020), there was an increasing trend for O_3. Based on Eq. (1), the year at which the maximum of the fitted curve occurred ($year_{max}$) is obtained as follows (Parrish et al. 2019, 2020).

Table 1. Three parameters determined by the fitted curve at three remote sites in Japan and other sites taken from the previous studies.

Site	a (ppbv)	b (ppbv/year)	c ($\times 10^{-3}$ ppbv/year^2)	$year_{max}$	Reference
Minamitorishima (MNM)	28.0 ± 1.1 (27.8 ± 1.1)*	−0.28 ± 0.21 (−0.28 ± 0.21)*	+35 ± 42 (+44 ± 39)*	—	This study
Yonagunijima (YON)	40.3 ± 1.2 (40.2 ± 1.2)	−0.15 ± 0.50 (−0.17 ± 0.48)	−12 ± 76 (−8 ± 69)	—	This study
Ryori (RYO)	38.9 ± 0.8* (38.8 ± 0.7)*	+0.24 ± 0.10* (+0.25 ± 0.10)*	−12 ± 19* (−8 ± 18)*	2009.5 ± 7.3	This study
Pacific marine boundary layer	32.9 ± 1.1	+0.14 ± 0.10	−25 ± 11	2002.8 ± 2.2	Parrish et al. (2020)
Mace Head, Ireland	40.1 ± 0.8 39.8 ± 0.6	+0.34 ± 0.07 +0.35 ± 0.06	−23 ± 8 −20 ± 6	2007 ± 6 2008.8 ± 3.2	Derwent et al. (2018) Parrish et al. (2020)
Mt. Waliguan, China	49.5 ± 0.4	+0.19 ± 0.05	+3 ± 7	—	Parrish et al. (2020)

Note: The parentheses indicate the result of curve fitting including the data from 2020. Significance level of $p < 0.05$ for the curve fitting is shown by *. $year_{max}$ is not derived and shown by – because the value of c is positive at Minamitororishima (MNM) and the values of both b and c are negative at Yonagunijima (YON).

Table 2. Top three lowest values of the observed background O_3 concentration at three remote sites in Japan from the 1990s to 2020.

Site	Statistical metrics	1st	2nd	3rd
Minamitorishima (MNM)	75th percentile (Q3)	34.50 (2009)	**35.25 (2020)**	36.50 (2016)
	50th percentile (Q2)	20.50 (2007)	**21.50 (2020)**	21.90 (2011)
	25th percentile (Q1)	11.40 (2009)	11.90 (2007)	**13.00 (2020)**
	Mean	23.56 (2009)	**24.31 (2020)**	25.26 (2007)
Yonagunijima (YON)	75th percentile (Q3)	**48.30 (2020)**	48.50 (2015, 2016)	48.60 (2014)
	50th percentile (Q2)	40.60 (2016)	40.70 (2015)	40.80 (2014)
	25th percentile (Q1)	**22.90 (2020)**	23.80 (2005, 2010, 2016)	23.90 (2007, 2008, 2009, 2015)
	Mean	**37.29 (2020)**	37.81 (2005)	37.89 (2010)
Ryori (RYO)	75th percentile (Q3)	41.60 (2001)	41.70 (1993)	**42.10** (1992, **2020**)
	50th percentile (Q2)	35.50 (2001)	35.60 (1993)	36.00 (1992)
	25th percentile (Q1)	27.60 (1993)	28.70 (2016)	29.20 (2001)
	Mean	34.80 (1993)	35.30 (1992)	35.56 (2001)

Note: The parentheses indicate the corresponding year and all units for O_3 concentration are ppbv. The year 2020 is shown in bold font.

$$year_{max} = -b/2c + 2000 \quad (2)$$

At RYO, where there was an increasing trend for O_3, $year_{max}$ estimated from Eq. (2) was 2009.5 ± 7.3. This peak in the mid-2000s at RYO calculated here agreed well with the results from over the Northern Hemisphere (Table 1 and detailed in Parrish et al. 2020). In Fig. 2, the analysis including 2020 are also overlayed, and the results for the fitted curve are also listed in Table 1. The spread of COVID-19 strongly affected the air quality in 2020 (Liu et al. 2020; Wang et al. 2021; Itahashi et al. 2022). The results for the three parameters were affected by including the year 2020, and the decrease in the values of parameters a and b suggested a further decreasing trend for O_3.

Finally, we focus on the change in O_3 concentration in 2020 during COVID-19. O_3 concentration at three remote sites showed year-to-year variation (Figs. 2 and 3). Table 2 lists the top three lowest values of the statistical metrics (75th, 50th, and 25th percentiles and arithmetic mean) at each site. Although lower O_3 concentrations occurred in different years at each site, 2020 showed lower concentrations at all three sites (RYO remarked 4th or 5th lowest concentration, see also Table 3). This result suggested that there was a common factor causing the lower concentration in 2020.

From the emission inventory estimation, anthropogenic NO_x emissions in 2020 declined 30%–40% (greater than anthropogenic VOC emissions decline) during the lockdown period (Forster et al. 2020; Zheng et al. 2021). Thus, O_3 concentrations in urban areas generally increased because of the weakening of O_3 titration by large NO_x emission reductions based on a literature review of urban air pollution during the COVID-19 lockdown globally (Gkatzelis et al. 2021). Similarly, increased O_3 concentrations were reported in urban areas (e.g., Tokyo metropolitan area) of Japan (Damiani et al. 2022, 2024). In contrast to these features over urban areas, the background O_3 concentration at Mace Head, Ireland decreased more than concentrations derived considering recent long-term decreasing trends (Parrish et al.

Table 3. Statistical metrics of observed background O_3 concentration at three remote sites in Japan from the 1990s to 2019 and for 2020.

Site	Statistical metrics	O_3 concentration averaged over 1990s to 2019 (ppbv)	O_3 concentration in 2020 (ppbv)
Minamitorishima (MNM)	75th percentile (Q3)	40.80	35.25 (−5.55)
	50th percentile (Q2)	25.90	21.50 (−4.40)
	25th percentile (Q1)	14.80	13.00 (−1.80)
	Mean	27.76	24.31 (−3.45)
Yonagunijima (YON)	75th percentile (Q3)	50.20	48.30 (−1.90)
	50th percentile (Q2)	41.90	41.20 (−0.70)
	25th percentile (Q1)	24.40	22.90 (−1.50)
	Mean	38.68	37.29 (−1.39)
Ryori (RYO)	75th percentile (Q3)	45.50	42.10 (−3.40)
	50th percentile (Q2)	38.70	36.60 (−2.10)
	25th percentile (Q1)	32.50	31.00 (−1.50)
	Mean	38.90	36.31 (−2.59)

Note: Parentheses indicate the difference between 2020 and from the 1990s to 2019.

2022). This finding was consistent with our analyses using the fitting curve shown in Fig. 3. The global total tropospheric O_3 burden decreased dramatically by about 2% in May and June 2020 (Miyazaki et al. 2021). Based on these results, we further analyzed the frequency density of O_3 concentration before COVID-19 (1990s to 2019) and in 2020 (Fig. 4). The frequency density shifted to a lower concentration in 2020 compared with the 1990s to 2019. The statistical metrics (75th, 50th, and 25th percentiles and arithmetic mean) are listed in Table 3. All metrics showed a decrease in 2020 compared with the 1990s to 2019 (Fig. 2), and the changes were greater in the higher concentration range (75th percentile rather than 25th percentile). The analysis of 2020 clarified the decrease in background O_3 concentration at remote sites in Japan. The decrease in O_3 concentration could be partly within the year-to-year variation; however, one possible factor causing this decreasing background O_3 concentration is the unprecedented anthropogenic emission reduction resulting from the COVID-19 pandemic in 2020.

4. Conclusion

The long-term near-30-year trend of background O_3 concentration at three remote sites in Japan was analyzed based on a quadratic polynomial fitted curve. The fitted curve results revealed that background O_3 concentration at these remote sites has been changing by ±0.3 ppbv/year over the 30 years from the 1990s to 2020. Our study revealed that MNM (24.28°N, 153.98°E) in easternmost Japan and YON (24.47°N, 123.02°E) in westernmost Japan showed a decreasing trend for O_3. RYO (39.03°N, 141.82°E) in northeast Japan showed an increasing trend for O_3, with its peak in 2009 and a subsequent decrease. This peak-out O_3 trend was consistent with other analyses of the mid-latitudes in the Northern Hemisphere (40°N–55°N). The unique continuously decreasing background O_3 concentration at a latitude of 20°N should

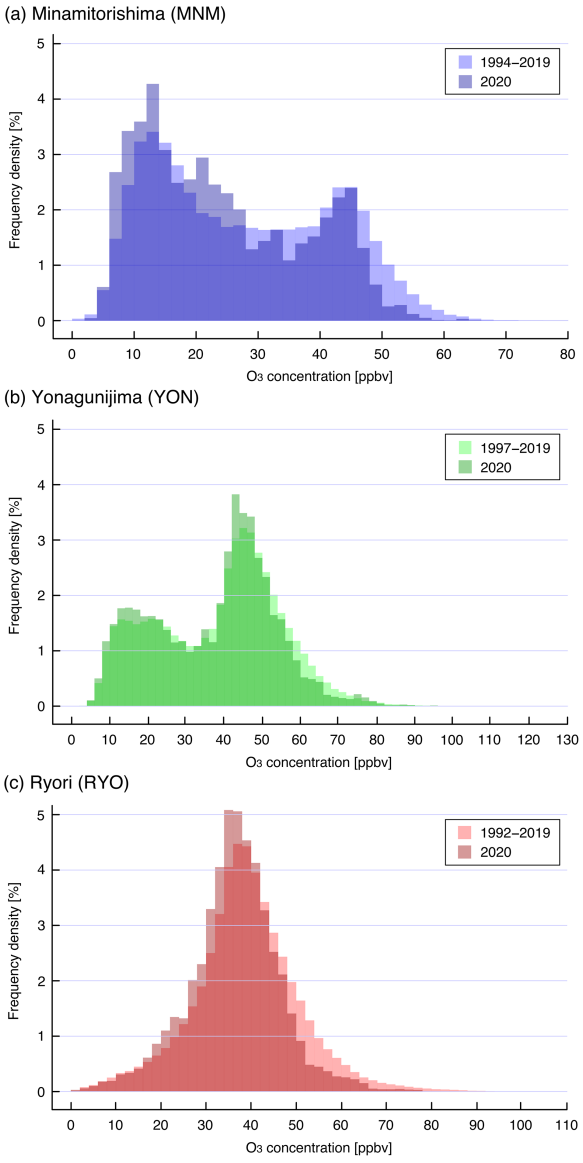

Fig. 4. Frequency density diagram of O_3 concentration at (a) Minamitorishima, (b) Yonagunijima, and (c) Ryori. The light colors indicate the data from the 1990s to 2019 and the dark colors indicate the data for 2020.

be studied further with the available dataset. Detailed analyses for 2020 clarified that background O_3 concentration decreased in all concentration ranges at all three remote sites in Japan, possibly because of the anthropogenic emission reduction owing to the COVID-19 pandemic.

Acknowledgements

This study was supported by the Environment Research and Technology Development Fund (JPMEERF20215005, JPMEERF20222001, JPMEERF20235M01, and JPMEERF20235R02) of the Environmental Restoration and Conservation Agency of Japan, provided by the Ministry of Environment, Japan, JSPS KAKENHI Grant Number JP23K25011. The author is grateful to the Japan Meteorological Agency (JMA) for providing the surface O_3 measurement dataset available from https://www.data.jma.go.jp/ghg/info_ghg_e.html.

Edited by: S. Morimoto

References

Akimoto, H., H. Mukai, M. Nishikawa, K. Murano, S. Hatakeyama, C.-M. Liu, M. Buhr, K. J. Hsu, D. A. Jaffe, L. Zhang, R. Honrath, J. T. Merrill, and R. E. Newell, 1996: Long-range transport of ozone in the East Asian Pacific rim region. *J. Geophys. Res.*, **101**, 1999–2010, doi:10.1029/95JD00025.

Chatani, S., H. Shimadera, S. Itahashi, and K. Yamaji, 2020: Comprehensive analyses of source sensitivities and apportionments of $PM_{2.5}$ and ozone over Japan via multiple numerical techniques. *Atmos. Chem. Phys.*, **20**, 10311–10329, doi:10.5194/acp-20-10311-2020.

Chatani, S., K. Kitayama, S. Itahashi, H. Irie, and H. Shimadera, 2023: Effectiveness of emission controls implemented since 2000 on ambient ozone concentrations in multiple timescales in Japan: An emission inventory development and simulation study. *Sci. Total Environ.*, **894**, 165058, doi:10.1016/j.scitotenv.2023.165058.

Crippa, M., D. Guizzardi, M. Muntean, E. Schaaf, F. Dentener, J. A. van Aardenne, S. Monni, U. Doering, J. G. J. Oliver, V. Pagliari, and G. Janssens-Maenhout, 2018: Gridded emissions of air pollutants for the period 1970–2012 within EDGAR v4.3.2. *Earth Syst. Sci. Data*, **10**, 1987–2013, doi:10.5194/essd-10-1987-2018.

Crippa, M., D. Guizzardi, T. Butler, T. Keating, R. Wu, J. Kaminski, J. Kuenen, J. Kurokawa, S. Chatani, T. Morikawa, G. Pouliot, J. Racine, M. D. Moran, Z. Klimont, P. M. Manseau, R. Mashayekhi, B. H. Henderson, S. J. Smith, H. Suchyta, M. Muntean, E. Solazzo, M. Banja, E. Schaaf, F. Pagani, J.-H. Woo, J. Kim, F. Monforti-Ferrario, E. Pisoni, J. Zhang, D. Niemi, M. Sassi, T. Ansari, and K. Foley, 2023: The HTAP_v3 emission mosaic: Merging regional and global monthly emissions (2000–2018) to support air quality modeling and policies. *Earth Syst. Sci. Data.*, **15**, 2667–2694, doi:10.5194/essd-15-2667-2023.

Damiani, A., H. Irie, D. A. Belikov, S. Kaizuka, H. M. S. Hoque, and R. R. Cordero, 2022: Peculiar COVID-19 effects in the Greater Tokyo Area revealed by spatiotemporal variabilities of tropospheric gases and light-absorbing aerosols. *Atmos. Chem. Phys.*, **22**, 12705–12726, doi:10.5194/acp-22-12705-2022.

Damiani, A., H. Irie, D. Belikov, R. R. Cordero, S. Feron, and N. N. Ishizaki, 2024: Air quality and urban climate improvements in the world's most populated region during the COVID-19 pandemic. *Environ. Res. Lett.*, **19**, 034023, doi:10.1088/1748-9326/ad25a2.

Derwent, R. G., A. J. Manning, P. G. Simmonds, T. G. Spain, and S. O'Doherty, 2018: Long-term trends in ozone in baseline and European regionally-polluted air at Mace Head, Ireland over a 30-year period. *Atmos. Environ.*, **179**, 279–287, doi:10.1016/j.atmosenv.2018.02.024.

Forster, P. M., H. I. Forster, M. J. Evans, M. J. Gidden, C. D. Jones, C. A. Keller, R. D. Lamboll, C. L. Quéré, J. Rogelj, D. Rosen, C.-F. Schleussner, T. B. Richardson, C. J. Smith, and S. T. Turnock, 2020: Current and future global climate impacts resulting from COVID-19. *Nat. Climate Change*, **10**, 913–919, doi:10.1038/s41558-020-0883-0.

Gkatzelis, G. I., J. B. Gilman, S. S. Brown, H. Eskes, A. R. Gomes, A. C. Lange, B. C. McDonald, J. Peischl, A. Petzold, C. R. Thompson, and A. Kiendler-Scharr, 2021: The global impacts of COVID-19 lockdowns on urban air pollution: A critical review and recommendations. *Elem. Sci. Anth.*, **9**, 00176, doi:10.1525/elementa.2021.00176.

Guerova, G., I. Bey, J.-L. Attié, R. V. Martin, J. Cui, and M. Sprenger, 2006: Impact of transatlantic transport episodes on summertime ozone in Europe. *Atmos. Chem. Phys.*, **6**, 2057–2072, doi:10.5194/acp-6-2057-2006.

Itahashi, S., I. Uno, and S. Kim, 2013: Seasonal source contributions of tropospheric ozone over East Asia based on CMAQ-HDDM. *Atmos. Environ.*, **70**, 204–217, doi:10.1016/j.atmosenv.2013.01.026.

Itahashi, S., H. Hayami, and I. Uno, 2015: Comprehensive study of emission source contributions for tropospheric ozone formation over East Asia. *J. Geophys. Res.: Atmos.*, **120**, 331–358, doi:10.1002/2014JD022117.

Itahashi, S., R. Mathur, C. Hogrefe, S. L. Napelenok, and Y. Zhang, 2020: Modeling trans-Pacific transport on tropospheric ozone using hemispheric CMAQ during April 2010 - Part 2: Examination of emission impacts based on the higher-order decoupled direct method. *Atmos. Chem. Phys.*, **20**, 3397–3413, doi:10.5194/acp-20-3397-2020.

Itahashi, S., J. Kurokawa, T. Ohara, I. Uno, and S.-i. Fujita, 2021: The 36-year historical variation of precipitation chemistry during 1976–2011 at Ryori WMO-GAW station in Japan. *SOLA*, **17**, 184–190, doi:10.2151/sola.2021-032.

Itahashi, S., Y. Yamamura, Z. Wang, and I. Uno, 2022: Returning long-range $PM_{2.5}$ transport into the leeward of East Asia in 2021 after Chinese economic recovery from the COVID-19 pandemic. *Sci. Rep.*, **12**, 5539, doi:10.1038/s41598-022-09388-2.

Itahashi, S., 2023: Severe level of photochemical oxidants (O_x) over the western coast of Japan during autumn after typhoon passing. *Sci. Rep.*, **13**, 16369, doi:10.1038/s41598-023-43485-0.

Itahashi, S., Y. Terao, K. Ikeda, and H. Tanimoto, 2024: Source identification of carbon monoxide over the greater Tokyo area: Tower measurement network and evaluation of global/regional model simulations at different resolutions. *Atmos. Environ.: X*, **23**, 100284, doi:10.1016/j.aeaoa.2024.100284.

JMA, 2024: Greenhouse gases. Japan Meteorological Agency (Available online at: https://www.data.jma.go.jp/ghg/info_ghg_e.html, accessed 15 October 2024).

Kawano, N., T. Nagashima, and S. Sugata, 2022: Changes in seasonal cycle of surface ozone over Japan during 1980–2015. *Atmos. Environ.*, **279**, 119108, doi:10.1016/j.atmosenv.2022.119108.

Kurokawa, J., and T. Ohara, 2020: Long-term historical trends in air pollutant emissions in Asia: Regional Emission inventory in ASia (REAS) version 3. *Atmos. Chem. Phys.*, **20**, 12761–12793, doi:10.5194/acp-20-12761-2020.

Lee, S., H. Akimoto, H. Nakane, S. Kurnosenko, and Y. Kinjo, 1998: Lower tropospheric ozone trend observed in 1989–1997 at Okinawa, Japan. *Geophys. Res. Lett.*, **25**, 1637–1640, doi:10.1029/98GL01224.

Liu, F., A. Page, S. A. Strode, Y. Yoshida, S. Choi, B. Zheng, L. K. Lamsal, C. Li, N. A. Krotkov, H. Eskes, R. van der A, P. Veefkind, P. F. Levelt, O. P. Hauser, and J. Joiner, 2020: Abrupt decline in tropospheric nitrogen dioxide over China after the outbreak of COVID-19. *Sci. Adv.*, **6**, eabc2992, doi:10.1126/sciadv.abc2992.

Mathur, R., D. Kang, S. L. Napelenok, J. Xing, C. Hogrefe, G. Sarwar, S. Itahashi, and B. H. Henderson, 2022: How have divergent global emission trends influenced long-range transported ozone to North America? *J. Geophys. Res.: Atmos.*, **127**, e2022JD036926, doi:10.1029/2022JD036926.

Miyazaki, K., K. Bowman, T. Sekiya, M. Takigawa, J. L. Neu, K. Sudo, G. Osterman, and H. Eskes, 2021: Global tropospheric ozone responses to reduced NO_x emissions linked to the COVID-19 worldwide lockdowns. *Sci. Adv.*, **7**, eabf7460, doi:10.1126/sciadv.abf7460.

Nagashima, T., K. Sudo, H. Akimoto, J. Kurokawa, and T. Ohara, 2017: Long-term change in the source contribution to surface ozone over Japan. *Atmos. Chem. Phys.*, **17**, 8231–8246, doi:10.5194/acp-17-8231-2017.

Parrish, D. D., K. S. Law, J. Staechelin, R. Derwent, O. R. Cooper, H. Tanimoto, A. Volz-Thomas, S. Gilge, H.-E. Scheel, M. Steinbacher, and E. Chan, 2012: Long-term changes in lower tropospheric baseline ozone concentrations at northern mid-latitudes. *Atmos. Chem. Phys.*, **12**, 11485–11504, doi:10.5194/acp-12-11485-2012.

Parrish, D. D., R. G. Derwent, S. O'Doherty, and P. G. Simmonds, 2019: Flexible approach for quantifying average long-tern changes and seasonal cycles of tropospheric trace species. *Atmos. Meas. Tech.*, **12**, 3383–3394, doi:10.5194/amt-12-3383-2019.

Parrish, D. D., R. G. Derwent, W. Steinbrecht, R. Stübi, R. Van Malderen, M. Steinbacher, T. Trickl, L. Ries, and X. Xu, 2020: Zonal similarity of long-term changes and seasonal cycles of baseline ozone at northern midlatitudes. *J. Geophys. Res.: Atmos.*, **125**, e2019JD031908, doi:10.1029/2019JD031908.

Parrish, D. D., R. G. Derwent, I. C. Faloona, and C. A. Mims, 2022: Technical note: Northern midlatitude baseline ozone – Long-term changes and the COVID-19 impact. *Atmos. Chem. Phys.*, **22**, 13423–13430, doi:10.5194/acp-22-13423-2022.

Seinfeld, J. H., and S. N. Pandis, 2016: *Atmospheric Chemistry and Physics: From Air Pollution to Climate Change, Third Edition*. John Wiley & Sons.

Sunwoo, Y., G. R. Carmichael, and H. Ueda, 1994: Characteristics of background surface ozone in Japan. *Atmos. Environ.*, **28**, 25–37.

Tanimoto, H., 2009: Increase in springtime tropospheric ozone at a mountainous site in Japan for the period 1998–2006. *Atmos. Environ.*, **43**, 1358–1363, doi:10.1016/j.atmosenv.2008.12.006.

Vingarzan, R., 2004: A review of surface ozone background levels and trends. *Atmos. Environ.*, **38**, 3431–3442, doi:10.1016/j.atmosenv.2004.03.030.

Wang, Z., I. Uno, K. Yumimoto, S. Itahashi, X. Chen, W. Yang, and Z. Wang, 2021: Impacts of COVID-19 lockdown, Spring Festival and meteorology on the NO_2 variations in early 2020 over China based on in-situ observations, satellite retrievals and model simulations. *Atmos. Environ.*, **244**, 117972, doi:10.1016/j.atmosenv.2020.117972.

Zheng, B., Q. Zhang, G. Geng, C. Chen, Q. Shi, M. Cui, Y. Lei, and K. He, 2021: Changes in China's anthropogenic emissions and air quality during the COVID-19 pandemic in 2020. *Earth Syst. Sci. Data*, **13**, 2895–2907, doi:10.5194/essd-13-2895-2021.